KERNEL DENSITY ANALYSIS AS A TOOL FOR PREDICTING LOCATIONS OF FUTURE VOLCANIC ERUPTIONS IN IMDR REGIO, VENUS. Rebecca M. Hahn[1] and Paul K. Byrne[1] , [1]Department of Earth and Planetary Sciences, Washington University in St. Louis, St. Louis, MO 63130 (h.rebeccahahn@wustl.edu)

Introduction: The recent discovery of an active volcano on Venus [1] has fueled the search for additional evidence for active volcanism, with a particular emphasis on regions predicted to host mantle uwellings based on geological and geophysical observations [2, 3]. In this study, we analyzed the spatial distribution of volcanoes within Imdr Regio, a ~1,300 km-diameter volcanic rise located in the southwest quadrant of Venus hypothesized to be underlain by a large mantle upwelling [4–6]. Imdr Regio hosts a 200 km diameter edifice, Idunn Mons, that is thought to be geologically recently active based on high-emissivity anomalies from ESA's Venus Express Visible and Infrared Thermal Imaging Spectrometer (VIRTIS) [3, 5, 6].

Analyzing the spatial distribution and concentration of edifices within Imdr Regio can provide valuable insight into the size and shape of the underlying magma source(s), the mechanism of magma production, and the states of stress in the crust [e.g., 7–9]. Furthermore, the distribution of volcanoes can be used to predict probable locations of future vents based solely on the locations of past eruptions [10–13]. Our goal is to use our recent map of volcanoes on Venus [14] to identify areas in Imdr Regio where, applying kernel density analysis [c.f., 13], future volcanoes have a high probability of forming.

Data: We delineated the Imdr Regio study region by generating 100 km-contour lines from the Magellan global altimetry dataset [15] and extracting that contour which fully encompassed the regional topographic high that broadly corresponded to Imdr Regio (~1,300 km) [4] (white polygon in **Fig. 2**). With our previously developed global catalog of volcanoes on Venus [14] (**Fig 1**), we extracted all the volcanoes ≤63 km in diameter that fell within the Imdr Regio contour boundary. This diameter value was informed by our earlier analysis, in which we identified two distinct distributions of volcanoes on Venus based on statistical mixture modeling: those >63 km in diameter and those ≤63 km in diameter [14]. For our kernel density analysis here, we included 367 volcanoes ≤63 km in diameter that fall within the contour boundary of Imdr Regio. We note that there is only one volcano >63 km within Imdr Regio, Idunn Mons, which is too small of a population to conduct a spatial analysis for locations where future large (i.e., >63 km-diameter) volcanoes could form.

Methods: Kernel density functions are non-parametric density estimation tools [16] that have been used extensively in the planetary community to examine, for instance, volcano spatial density on Mars [e.g., 13, 17] and on Venus [e.g., 18]. Here, we utilized the freely available R statistical package "ks" [19] to perform our kernel density analyses.

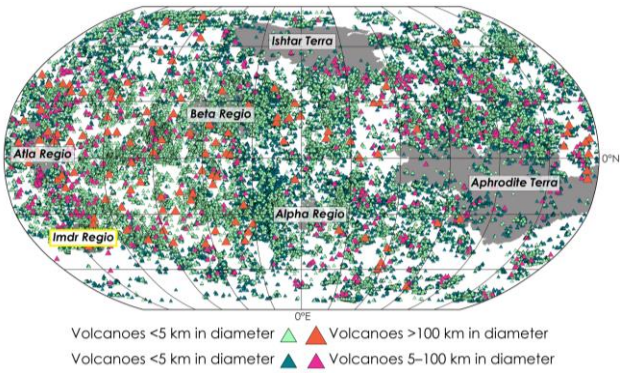

Figure 1: Our previously published global survey of volcanic edifices on Venus [14]. The outlines of major physiographic features are shown in grey for geographic context, with our study region, Imdr Regio, highlighted in yellow in the southwest quadrant. The map is in Robinson projection, centered at 0°E.

The kernel density function consists of two components, the probability density function (PDF) and the bandwidth value [13]. The PDF spreads probability away from the event (i.e., the volcano) based on the bandwidth and the shape of the kernel density function [13]. For this analysis, we employed two optimized bandwidth algorithms, the sum of the asymptotic mean-square error (SAMSE) and least-squares cross-validation (LSCV) [20]. Optimized bandwidth algorithms negate the subjectivity of arbitrarily selecting a bandwidth value, and instead provide an unbiased estimate of bandwidth elements based on distances between neighboring vents. Here, with the "ks" [19] package in R, we employed a two-dimensional, direction-varying elliptical kernel bandwidth to calculate the variation in spatial density for volcanoes ≤63 km in diameter within Imdr Regio using each of the two optimized bandwidth algorithms, yielding two volcano spatial density maps.

Results: Kernel density maps produced by the SAMSE and LSCV algorithms (**Fig 2**) produce differently sized regions of high volcano spatial density, but both reveal nearly identical concentrations of volcanoes in the northwestern portion of Imdr Regio. Differences in the extents of the resulting kernel density maps are because of variations in kernel sizes and the criterion being optimized in each algorithm. For example, the SAMSE algorithm produced an elliptical kernel with a semi-major axis rotated <1° to the N–NE and that measures ~0.9 km in the N–S direction and ~1.5 km in the E–W direction. In contrast, the LSCV kernel is smaller, measuring 0.2 km in the N–S direction and 0.4 km in the E–W direction, and with a semi-major axis oriented <1° to the N–NW. Generally, the LSCV method can result in narrow and elongated kernels that have a tendency to overfit the data, whereas the

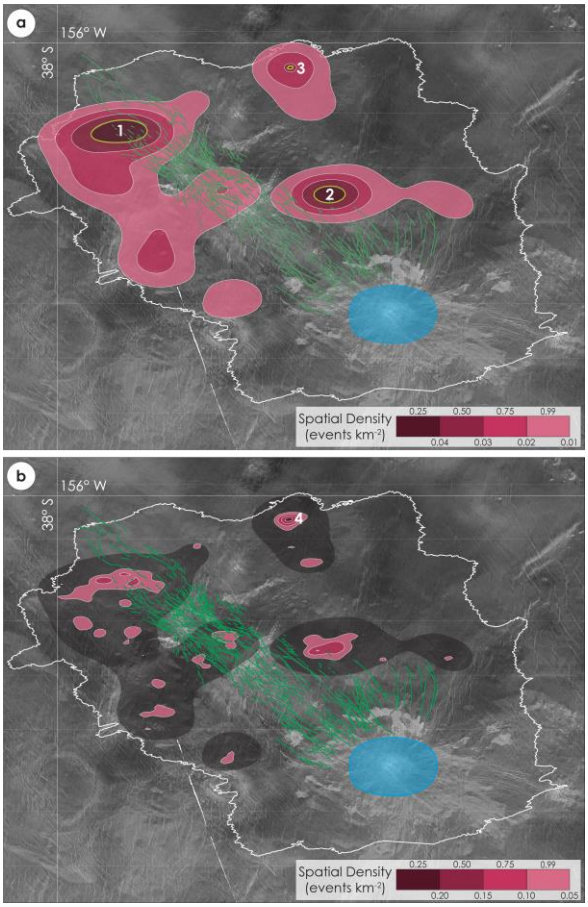

Figure 2: Spatial density estimates for volcanoes ≤63 km in diameter within the Imdr Regio boundary (white polygon) utilizing the sum of the asymptotic mean-square error (a) and least-squares cross-validation (b) bandwidth optimization algorithms. Regions with statistically highest likelihood of new vents forming are outlined in yellow in map (a). Contours are shown at 25th, 50th, 75th, and 99th percentiles, with high-volcano-spatial-density regions (99th percentile) numbered 1–4. Grey regions in map (b) show the overlap between high-volcano-spatial-density regions generated by the SAMSE algorithm, for comparison. The blue oval demarcates Idunn Mons, and green lines represent of Olapa Chasma.

SAMSE method is more sensitive to individual vent locations and as a result may obscure fine-scale structure by underfitting the data [13, 21]. By comparing high-volcano-spatial-density regions produced by *both* maps (the darkest-pink regions in **Fig. 2**), we can reduce the errors associated with over- and under fitting the data that can occur with each algorithm individually.

Contours in **Fig 2** indicate the spatial quartile probability of where future volcanoes might form. Based on the distributions of existing vents, there is a 99% chance that a future vent in Imdr Regio will form within the regions bounded by the 0.01 contour (i.e., the 99th quartile, shown as the lightest pink region) in the volcano spatial density map generated by the SAMSE algorithm (**Fig 2a**), which also fully encompasses the regions predicted by the LSCV algorithm—which predicts smaller regions, but at higher volcano spatial densities (see grey regions in **Fig 2b**). Statistically, a new vent has the highest likelihood of forming within the 25% contour region in the SAMSE-generated volcano spatial density map (the yellow ellipses labeled 1–3 in **Fig 2a**), which also encompasses the highest-probability region predicted by the LSCV algorithm (the darkest-pink region labeled "4" in Fig **2b**).

Discussion & Outlook: The two most expansive regions of high-volcano-spatial-density distribution (the yellow ellipses labelled "1" and "2" in **Fig 2a**) overlap with a portion of Olapa Chasma (the green lines in **Fig 2**), a NW–SE-trending rift zone that extends from the NW portion of our study region down to the SE portion, where it intersects with Idunn Mons (the blue oval in **Fig 2**) [22]. The formation of the volcanoes already present within these high-spatial-density regions may be directly linked to the Olapa Chama, as feeder dykes can easily propagate through the fractures and cracks within the rift zone [23]. Future analysis of the dominant orientation or alignment of vents can provide insight into the regional stress field at the time of vent emplacement [23,24].

The high-volcano-spatial-density region not located along Olapa Chasma (the yellow ellipse labelled "3" in **Fig 2a**) is, on average, one-fifth the size of the other two regions. This smaller region is does not spatially intersect any nearby tectonic structures and is over 700 km away from Idunn Mons, and therefore existing volcanoes here could simply be the product of a low magma supply rate separate to any large-scale crustal extensional systems [25].

Developing a series of volcano spatial density maps at candidate hotspot regions across Venus (e.g., Alpha and Beta Regiones [2]) can facilitate the identification of areas that are statistically likely to see new volcanoes form. These maps can be used by future missions to Venus such as NASA's VERITAS and ESA's EnVision spacecraft to search for new volcanic constructs and help us answer fundamental questions related to the styles and eruption rates and frequencies of Venus volcanism.

References: [1] Herrick and Hensley (2023) Science, 379, 1205–1208. [2] Smrekar (1994) Icarus, 112, 2–26. [3] Smrekar et al. (2010) Science, 328, 605–608. [4] Stofan E.R. et al., (1995) JGR, 100, 23317–23327. [5] D'Inecco et al. (2017) PSS, 136, 25–33. [6] D'Inecco et al. (2021) PSJ, 2, 215. [7] Kear D. (1964) NZ JGG, 7, 22–24. [8] Connor C.B. (1990) JGR: SE, 95, 19395–19405. [9] Cañón-Tapia and Mendoza-Borunda (2014) JVGR, 281, 53–69. [10] Connor and Connor (2009) *Volc. & tec. hazard assessment for nuclear facilities, 346368.* [11] Germa et al. (2013) Bull. Volc. 75, 1–14. [12] Tadini et al. (2017) JGRSE, 122, 4357–4376. [13] Connor et al. (2019) Stats in Volc., 4, 1–25. [14] Hahn and Byrne (2023) JGRP, 128, e2023JE007753. [15] Ford (1992) Global data record topographic V1.0 [Dataset]. NASA Planetary Data System. [16] Silverman (1986) Density est. for stats and data analysis. [17] Richardson (2013) USF, 1–24. [18] Cañón-Tapia (2014) JVGR, 281, 70– 84. [19] Duong (2007) JNS, 15, 17–30. [20] Duong T. & Hazelton M. (2003) JNS, 15, 17–30. [21] Bebbington (2013) JVGR, 252, 14–28. [22] D'Incecco et al. (2020) EPSL, 546, 116410. [23] Le Corvec et al. (2013) ESR, 124, 96–114. [24] Cebriá et al. (2011) JVGR, 201, 73–82. [25] Crumpler et al. (1997) Venus II, 697–756.